A Model-Based Estimator of Engine Cylinder Pressure Imbalance for Combustion Feedback Control Applications

Ahmed Al-Durra, Lisa Fiorentini, Marcello Canova and Stephen Yurkovich

Abstract— One of the principal issues of low-temperature combustion modes is caused by the imbalances in the distribution of air and EGR across the cylinders, which affects the combustion process. Cylinder to cylinder variations lead to imbalances in the cylinder pressure, indicated torque, exhaust gas thermodynamic conditions and emissions.

In principle, a cylinder-by-cylinder control approach could compensate for air, residuals and charge temperature imbalance. However, in order to fully benefit from closed-loop combustion control, a feedback from each engine cylinder would be necessary to reconstruct the pressure trace. Therefore, cylinder imbalance is an issue that can be detected only in a laboratory environment, wherein each engine cylinder is instrumented with a dedicated pressure transducer.

This paper describes the framework and preliminary results of a model-based estimation approach to predict the individual pressure traces in a multi-cylinder engine from the output of a crankshaft speed sensor. The objective of the estimator is to reconstruct the complete pressure trace during an engine cycle with sufficient accuracy to allow for detection of cylinder to cylinder imbalances. Starting from a model of the engine crankshaft dynamics, a sliding mode observer is designed to estimate the cylinder pressure from the crankshaft speed fluctuation measurement. The results obtained by the estimator are compared with experimental data obtained on a four-cylinder Diesel engine.

I. INTRODUCTION

Over the past decade, Diesel engine technology has rapidly evolved due to the significant advances in turbocharging, fuel injection systems, combustion optimization and aftertreatment technology. However, well designed and calibrated control strategies must be implemented to manage the fueling system and air handling system, while relying on a restricted set of sensors due to cost limitations [1].

Conventional Diesel engines typically operate in open loop with respect to combustion. As emissions and diagnostic regulations have become more stringent, the possibility of closed-loop combustion control has recently gained interest. In particular, the possibility of controlling the individual fuel injectors could help compensate for several sources of variability, such as the air and residual mass imbalance that occurs between cylinders and leads to differences in cylinder pressure traces, engine torque and emissions [2], [3]. However, in order to fully benefit from closed-loop combustion control, it is necessary to obtain feedback from each engine cylinder to reconstruct the pressure trace [4].

Ahmed Al-Durra is with the Department of Electrical Engineering, The Petroleum Institute, Abu Dhabi, UAE al-durra.1@osu.edu

Lisa Fiorentini, Marcello Canova and Stephen Yurkovich are with the Center for Automotive Research, The Ohio State University, Columbus, OH, 43212 USA fiorentini.2@osu.edu, canova.1@osu.edu, yurkovic@ece.osu.edu

Processing cylinder pressure data for real-time applications requires several operations to be performed in order to eliminate the noise and offset issues associated with the output of piezoelectric transducers [5]. Furthermore, due to cost issues, the use of a dedicated piezoelectric transducer for each engine cylinder is today limited to laboratory testing.

For this reason, estimation techniques have been proposed to detect the in-cylinder pressure from other engine variables, such as the engine crankshaft speed fluctuations [6], [7]. Several methods have been proposed in the past, mainly for indicated torque, indicated mean effective pressure (*IMEP*) estimation and for combustion diagnostics, [6], [8]–[12]. Although the results presented in literature appear accurate for reconstructing the cylinder pressure and indicated torque during the combustion event, it is very difficult to design an estimator able to provide the cylinder pressure trace during an entire engine cycle (hence including the charge exchange phase), as well as to detect cylinder to cylinder pressure imbalances due to the air and EGR distribution.

This work proposes a model-based estimation methodology to obtain the pressure trace in a multi-cylinder Diesel engine with real-time capabilities and minimal sensor requirements. The outcome of this work is an algorithm intended for implementation into a closed-loop control system utilizing cylinder pressure feedback to compensate for imbalances due to air and EGR distribution across the cylinders.

II. STRUCTURE OF ENGINE TORQUE DYNAMICS MODEL

In its simplest form, the proposed estimation scheme utilizes the engine crankshaft speed sensor output to predict the pressure trace for each individual cylinder. Information from other sensors (such as the fuel mass flow rate and intake manifold pressure) is also used in the estimation algorithm.

Following the approach proposed in [5], a dynamic model of the in-cylinder processes based on the energy conservation principle is here applied to predict the cylinder pressure from intake valve closing to exhaust valve opening (IVC↦EVO). This model is here extended to an inline four-cylinder engine by properly phasing the combustion events based on the firing order of the engine and by approximating the pressure during the charge exchange phase of the cycle to a constant term. As a result, the pressures $p_{cyl,1}, \ldots, p_{cyl,4}$ of the four

cylinders are defined by the following equation:

$$\begin{cases} \dfrac{dp_{cyl,i}}{d\theta_i} + \dfrac{\gamma}{V_{cyl}}\dfrac{dV_{cyl}}{d\theta_i}p_{cyl,i} = \dfrac{\gamma-1}{V_{cyl}}\dfrac{dQ_n}{d\theta_i} & \text{if } \theta_{IVC} \leq \theta_i \leq \theta_{EVO} \\ \\ p_{cyl,i} = p_{IM} & \text{otherwise} \end{cases}$$
(1)

for $i = 1,\ldots,4$, where the crank angle is defined as:

$$\begin{aligned} \theta_1 &= rem(\theta,4\pi) & \text{Cylinder 1} \\ \theta_2 &= rem(\theta+\pi,4\pi) & \text{Cylinder 2} \\ \theta_3 &= rem(\theta+3\pi,4\pi) & \text{Cylinder 3} \\ \theta_4 &= rem(\theta+2\pi,4\pi) & \text{Cylinder 4} \end{aligned}$$

The apparent net heat release rate Q_n in Equation (1) accounts for the fuel energy released during the combustion and the heat losses due to heat transfer to the cylinder walls [13]. This term is estimated through the definition of an apparent fuel burning rate, which is modeled as a linear combinations of Wiebe functions calibrated on steady-state experimental data [14].

The cylinder pressure is used to calculate the instantaneous indicated torque $T_{ind,i}(\theta_i)$, acting on the crank arm [5], [12], [15]. In addition to the indicated torque, the the reciprocating inertia torque $T_{m,i}(\theta_i,\omega)$ and the engine friction torque $T_{fr}(\omega)$ must be modeled in order to determine the effective torque acting on the crank arm [13]. The above terms have been calculated as in [15].

Finally, a simple, one-degree of freedom model of the the rotational dynamics of the crankshaft system is defined by a torque balance, assuming the crankshaft as a rigid body:

$$\frac{d\omega(\theta)}{d\theta} = \sum_{i=1}^{4}\left(\frac{T_{ind,i}(\theta_i)+T_{m,i}(\theta_i,\omega)}{J_{eq}\omega}\right) - \frac{T_{fr}(\omega)+T_{load}}{J_{eq}\omega}$$
(2)

where J_{eq} is the equivalent inertia of the engine cranktrain.

In order to facilitate the design of the estimator, a simplification is introduced in the model. Specifically, it is assumed from here on that each torque pulse produced by a firing event causes a distinct fluctuations in crankshaft velocity and acceleration [16]–[18]. This allows one to decouple each cylinder pressure event which generates a torque contribution in Equation 2.

The complete engine cylinder pressure and crankshaft dynamics model given by Equations (1)-(2) can be converted to state-space form to facilitate the estimator design. To this end, the model is slightly approximated by assuming the reciprocating inertia torque as acting with the engine load as an external torque, and its value calculated from the estimated engine speed. Such approximation is accepted for a light-duty Diesel engine, where the indicated torque is an order of magnitude higher than the reciprocating inertia torque [15]. Furthermore, let:

- $A_{11}(\omega) = \dfrac{-k_{\omega_1}-k_{\omega_2}\omega}{J_{eq}\omega}$
- $A_{12}(\theta_i,\omega) = \dfrac{rA_p f(\theta_i)}{J_{eq}\omega}$

- $A_{22}(\theta_i,\omega) = -\dfrac{\gamma}{V_{cyl}(\theta_i)}\dfrac{dV_{cyl}(\theta_i)}{d\theta_i}$
- $N(\theta_i) = \dfrac{\gamma-1}{V_{cyl}(\theta_i)}\dfrac{dQ_n(\theta_i)}{d\theta}$
- $H(\theta,\omega) = \sum_{i=1}^{4}\dfrac{T_{m,i}-rA_p p_{amb}f(\theta_i)-T_{fr_0}-T_{load}}{J_{eq}\omega}$

These assumptions and notations lead to the following state representation form:

$$\begin{bmatrix} \dfrac{d\omega}{d\theta} \\ \\ \dfrac{dp_{cyl}}{d\theta} \end{bmatrix} = \begin{bmatrix} A_{11}(\omega) & A_{12}(\theta,\omega) \\ 0 & A_{22}(\theta,\omega) \end{bmatrix}\begin{bmatrix} \omega \\ p_{cyl} \end{bmatrix} + \begin{bmatrix} H(\theta,\omega) \\ N(\theta) \end{bmatrix}$$
(3)

where $p_{cyl} = [p_{cyl,1},\ldots,p_{cyl,4}]^T$ and

- $A_{12}(\theta,\omega) = [A_{12}(\theta_1,\omega),\ldots,A_{12}(\theta_4,\omega)]$
- $A_{22}(\theta,\omega) = diag\{A_{22}(\theta_1,\omega),\ldots,A_{22}(\theta_4,\omega)\}$
- $N(\theta) = diag\{N(\theta_1),\ldots,A_{22}(\theta_4)\}$

Finally, let $x = [\omega\ p_{cyl}^T]^T$ and

$$y = Cx = \begin{bmatrix} 1 & 0 \end{bmatrix}x = x_1 = \omega$$
(4)

In the above form, the model can be tested for observability, which is a necessary condition for the estimator design. To study the uniform observability of the system, the matrix

$$\Lambda(\theta) = \begin{bmatrix} C \\ \dot{C}+CA \end{bmatrix} = \begin{bmatrix} 1 & 0 \\ A_{11} & A_{12} \end{bmatrix}$$
(5)

must be of full rank for each angular position. The system described by Equation 3 results uniformly observable except at top dead center (TDC) and bottom dead center (BDC), where the condition $A_{12} = 0$ occurs [5]. This is physically reasonable, as the cylinder pressure has no effects on the crankshaft speed when the piston is located at its extreme positions.

III. DESIGN OF MULTI-CYLINDER PRESSURE ESTIMATOR

The cylinder pressure estimator for a multi-cylinder engine is implemented using a sliding mode observer (SMO), based on the plant model in Equation (3), and assuming the only measured variable is the engine instantaneous crankshaft speed. The choice of the sliding mode observer is motivated by the inherent robustness properties as well as the ability to deal with model uncertainties.

The state estimator is characterized by the following dynamics:

$$\frac{d\hat{y}}{d\theta} = A_{11}\hat{y}+A_{12}\hat{x}_2+H(\theta,\omega)+V$$
(6a)

$$\frac{d\hat{x}_2}{d\theta} = \overset{0}{\cancel{A_{21}\hat{y}}}+A_{22}\hat{x}_2+N(\theta)+LV$$
(6b)

where A_{mn} are the elements of matrix A in Equation 3, $V = K\ sign(\tilde{y})$, $\tilde{x}_2 = x_2-\hat{x}_2$, and the sliding surface $s = \tilde{y} = y-\hat{y}$.

The error model is given by:

$$\frac{d\tilde{y}}{d\theta} = A_{11}\tilde{y} + A_{12}\tilde{x}_2 - K\,sign(\tilde{y}) \tag{7a}$$

$$\frac{d\tilde{x}_2}{d\theta} = A_{22}\tilde{x}_2 - LK\,sign(\tilde{y}) \tag{7b}$$

The sliding mode gain K should be assigned so that the sliding mode will be enforced (i.e. $s\dot{s} < 0$). Therefore, K must be sufficiently large so that the sign of the right-hand side of Equation 7a is determined by the sign of the term $(-K\,sign(\tilde{y}))$.

To mitigate the control chattering associated to the sliding mode observer, the SMO gain can be designed as a function of the crank angle $K(\theta)$ so that it can satisfy the sign condition but with a small margin, as shown in Figure 1 [7]. Furthermore, a boundary layer is used for the sign function in a small neighborhood around the sliding surface ($s = 0$) to mitigate the chattering and smoothen the output by avoiding the discontinuity. The limits of the boundary layer must be chosen carefully so that the convergence rate of the error stays in a desirable range.
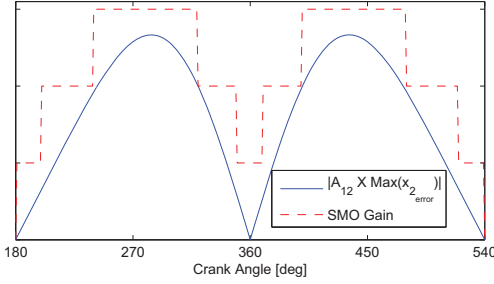

Fig. 1. A piecewise continuous sliding mode observer gain $K(\theta)$.

With the sliding mode enforced, the following can be obtained from the equivalent control principle:

$$\Rightarrow \tilde{y} = 0 \quad \Rightarrow \dot{\tilde{y}} = 0 \quad \Rightarrow V_{eq} = A_{12}\tilde{x}_2 \tag{8a}$$

$$\Rightarrow \frac{d\tilde{x}_2}{d\theta} = A_{22}\tilde{x}_2 - LA_{12}\tilde{x}_2 = (A_{22} - LA_{12})\tilde{x}_2 \tag{8b}$$

where V_{eq} is the *equivalent control*, which can be interpreted as the average of the control signal.

Finally, $L(\theta)$ is chosen such that $(A_{22} - LA_{12}) < 0$, which will make $\tilde{x}_2$ converge asymptotically to zero. Figure 2 shows that, with an appropriate choice of $L(\theta)$, the difference $A_{22} - L(\theta)A_{12}$ is always negative. Therefore, $\hat{x}_2$ should converge to $x_2 = p_{cyl}$.

IV. Design of Augmented Pressure Estimator

As designed, the SMO estimator predicts the cylinder pressure during the closed valve portion of the engine cycle. This design allows for predicting the engine *IMEP* and indicated torque, or for combustion diagnostics such as misfire detection [8]–[10], [12]. However, in order to obtain information on the in-cylinder charge composition, or detect imbalances in multi-cylinder engines, knowledge
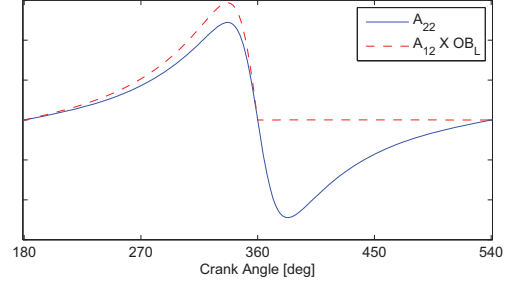

Fig. 2. A piecewise continuous observer gain $L(\theta)$.

of the pressure trace during the charge exchange portion of the cycle is required.

To overcome the issue of poor accuracy during the phases where two cylinder pressure traces overlap, the estimator is augmented by introducing an additional state that represents the torque produced by the prior cylinder in the sequence. To this end, define:

- $G = \dfrac{-k_1 - k_2\omega}{J\omega}$

- $g(\theta_i) = \dfrac{rA_pf(\theta_i)}{J\omega}$

- $M(\theta_i) = -\dfrac{\gamma}{V_{cyl}(\theta_i)}\dfrac{dV_{cyl}(\theta_i)}{d\theta_i}$

- $N(\theta_i) = \dfrac{\gamma - 1}{V_{cyl}(\theta_i)}\dfrac{dQ_n(\theta_i)}{d\theta_i}$

- $H(\theta,\omega) = \sum\dfrac{T_{m,i} - rA_pp_{amb}[f(\theta_i) - f(\theta_{i-1})] - T_{fr_0} - T_{load}}{J_{eq}\omega}$

where $i = 1,\ldots,4$ represents the firing cylinder.

The above assumptions render the model into the following state variable format:

$$\begin{bmatrix} \frac{dx_1}{d\theta} \\[4pt] \frac{dx_2}{d\theta} \\[4pt] \frac{dx_3}{d\theta} \end{bmatrix} = \begin{bmatrix} G & f(\theta_{i-1}) & f(\theta_i) \\ 0 & M(\theta_{i-1}) & 0 \\ 0 & 0 & M(\theta_i) \end{bmatrix} \begin{bmatrix} x_1 \\ x_2 \\ x_3 \end{bmatrix} + \begin{bmatrix} H(\theta_i) \\ N(\theta_{i-1}) \\ N(\theta_i) \end{bmatrix} \tag{9}$$

where $x_1 = \omega$, $x_2 = p_{i-1}$, $x_3 = p_i$, and

$$y = Cx = \begin{bmatrix} 1 & 0 & 0 \end{bmatrix} x = x_1 = \omega \tag{10}$$

Applying the SMO design, the state estimation is characterized by the following dynamics:

$$\frac{d\hat{x}_1}{d\theta} = G\hat{x}_1 + g(\theta_{i-1})\hat{x}_2 + g(\theta_i)\hat{x}_3 + H(\theta_i) + V \tag{11a}$$

$$\frac{d\hat{x}_2}{d\theta} = M(\theta_{i-1})\hat{x}_2 + N(\theta_{i-1}) + L_1V \tag{11b}$$

$$\frac{d\hat{x}_3}{d\theta} = M(\theta_i)\hat{x}_3 + N(\theta_i) + L_2V \tag{11c}$$

where $V = K\,sign(\tilde{y})$, and the sliding surface $s = \tilde{y} = y - \hat{y}$.

The error model is given by:

$$\frac{d\tilde{x}_1}{d\theta} = G\tilde{x}_1 + g(\theta_{i-1})\tilde{x}_2 + g(\theta_i)\tilde{x}_3 - K\,sign(\tilde{y}) \quad (12a)$$

$$\frac{d\tilde{x}_2}{d\theta} = M(\theta_{i-1})\tilde{x}_2 - L_1 K\,sign(\tilde{y}) \quad (12b)$$

$$\frac{d\tilde{x}_3}{d\theta} = M(\theta_i)\tilde{x}_3 - L_2 K\,sign(\tilde{y}) \quad (12c)$$

As shown above, the parameter K must be sufficiently large so that the sign condition is satisfied. Similarly, the chattering will be mitigated using the time varying gain and boundary layer techniques in a small range enough to avoid the convergence of error becoming sluggish.

With the sliding mode enforced, the following conclusions can be drawn using the equivalent control principle:

$$\tilde{y} = 0 \quad \Rightarrow \dot{\tilde{y}} = 0 \quad \Rightarrow V_{eq} = g(\theta_{i-1})\tilde{x}_2 + g(\theta_i)\tilde{x}_3 \quad (13)$$

Substituting the equivalence control into the error equation, the following state variable error model is obtained:

$$\begin{bmatrix} \frac{d\tilde{x}_2}{d\theta} \\ \frac{d\tilde{x}_3}{d\theta} \end{bmatrix} = \begin{bmatrix} M(\theta_{i-1}) - L_1 f(\theta_{i-1}) & -L_1 f(\theta_i) \\ -L_2 f(\Theta_{i-1}) & M(\theta_i) - L_2 f(\theta_i) \end{bmatrix} \begin{bmatrix} \tilde{x}_2 \\ \tilde{x}_3 \end{bmatrix} \quad (14)$$

where $L_1(\theta)$ and $L_2(\theta)$ are chosen such that the error system matrix is negative definite.

V. RESULTS AND ANALYSIS

The designed pressure estimator was validated on experimental data, obtained on a light-duty Diesel engine, whose main data are listed in Table I. Several steady-state engine operating conditions were acquired by varying the engine speed and torque. The crankshaft angular velocity was recorded with an optical transducer mounted on the engine harmonic dampener. The pressure trace of each individual cylinder was acquired for 70 consecutive engine cycles with a piezoelectric transducer. The signal was then low-pass filtered and pegged using the intake manifold pressure in order to obtain the final pressure measurement.

Engine Type	DI Diesel, inline four-cylinder
Displacement	2499 cm^3
Bore and Stroke	92, 94 mm
Compression Ratio	17.5:1
Connecting Rod Length	163 mm
IVO, IVC, EVO, EVC	$706^o, 246^o, 473^o, 31^o$
Max. Power	$105kW$ at $4000r/min$
Max. Torque	$320Nm$ at $2000r/min$

TABLE I

TEST ENGINE SPECIFICATIONS.

The validation study was conducted by comparing the estimator predictions to the measured in-cylinder pressure traces. Figure 3 shows the instantaneous crankshaft speed signal recorded from the engine at a nominally steady-state operating condition.

Figure 4 compares the pressure traces predicted by the pressure estimator without augmentation during one engine
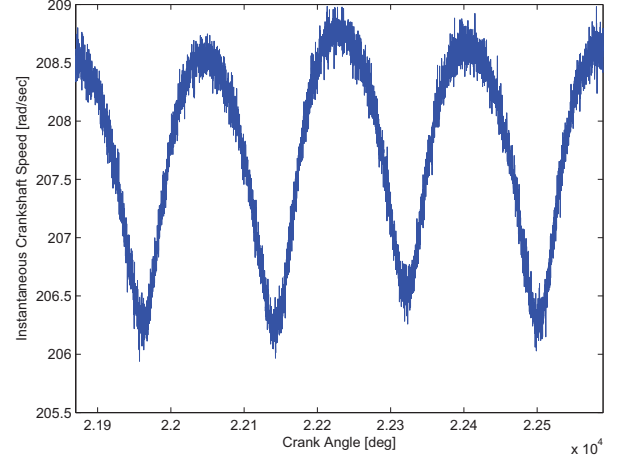

Fig. 3. Instantaneous engine crankshaft angular velocity signal during one engine cycle (Engine condition $N = 2000r/min, T = 40Nm$).

cycle with the experimental values, for the operating condition corresponding to the input engine speed in Figure 3. As expected, the estimator follows the pressure traces well during the closed-valve portion of the cycle, with the exception of a few points near top dead center. This behavior was explained by the singularity of the observability Grammian at this condition. The deviation in the estimated pressure trace could be mitigated by increasing the resolution of the speed signal.

Furthermore, a deviation of the estimate from the experimental data is evident when two pressure traces overlap. This follows from the assumption of considering only one cylinder pressure producing torque at each window, which causes the estimator to assume the positive torque from the previous cylinder as an equivalent pressure drop in the current acting cylinder, resulting in an estimation error.
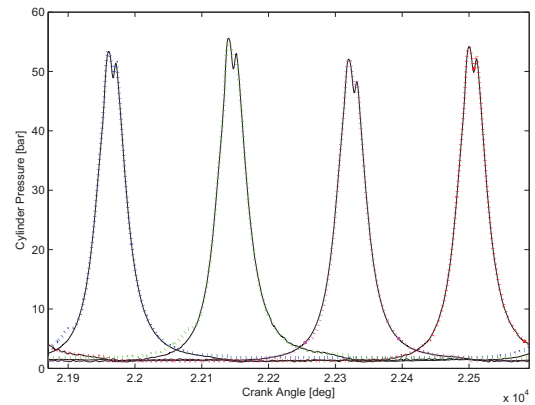

Fig. 4. Cylinder pressure traces predicted by the estimator without augmentation (dotted) and experimental data (solid) during one engine cycle. Left to right, the peaks represent cylinders 1, 3, 4, and 2 (Engine condition $N = 2000r/min, T = 40Nm$).

A set of indicative combustion metrics, namely the 50% burn rate location (CA_{50}), the peak pressure (P_{max}) and the *IMEP*, were calculated from the estimated pressure and compared to the experimental values. Figure 5 shows the value of the errors on the combustion metrics for 70 consecutive engine cycles using the data from cylinder 1. The SMO accurately estimates CA_{50} and P_{max}. On the other hand, a bias of 3% can be observed in the estimated *IMEP*, as a consequence of the drop in the estimated pressure during the intake and compression strokes, which makes the estimated *IMEP* slightly higher than the actual value. The results for the remaining cylinders are very similar, showing that the estimator is effective in capturing the differences in the pressure traces among the four cylinders.

Fig. 6. Cylinder pressure traces predicted by the augmented estimator (dotted) and experimental data (solid) during one engine cycle. Left to right, the peaks represent cylinders 1, 3, 4, and 2 (Engine condition $N = 2000r/min, T = 40Nm$).
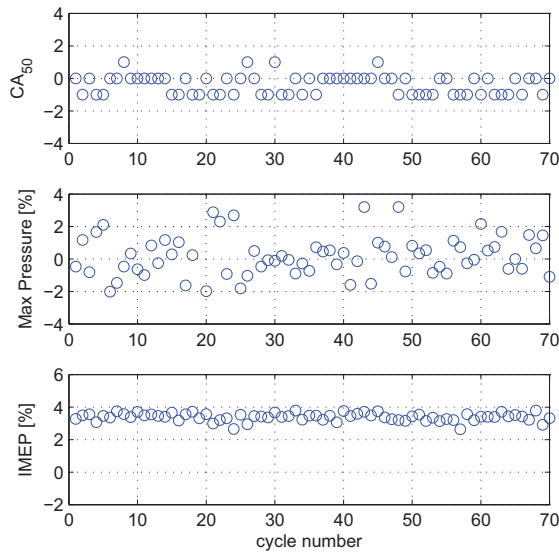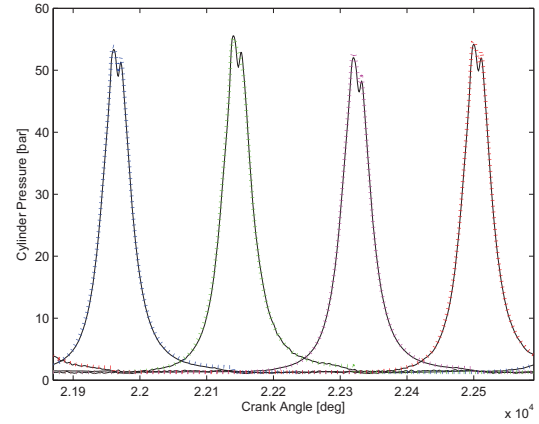

Fig. 5. Cycle by cycle error on the combustion metrics calculated from the cylinder 1 output of the estimator without augmentation (Engine condition $N = 2000r/min, T = 40Nm$).

Figure 6 shows the results of the augmented estimator in predicting the cylinder pressure traces during one engine cycle. Compared to Figure 4, an improved performance of the estimator in tracking the actual experimental pressure can now be observed. In particular, the deviation in the pressure estimation during the during the intake and early compression strokes is here completely eliminated by the introduction of the additional state to the model.

The improved accuracy can also be noticed in the combustion metrics. As shown in Figure 7, the augmented estimator leads to a considerably improved prediction of the engine *IMEP*. Furthermore, a slight improvement in the prediction of the cylinder peak pressure can also be observed, as a consequence of a better prediction of the cylinder pressure trace during the early portion of the compression stroke.

VI. CONCLUSIONS

This paper describes the preliminary results of a model-based estimation methodology to reconstruct the individual
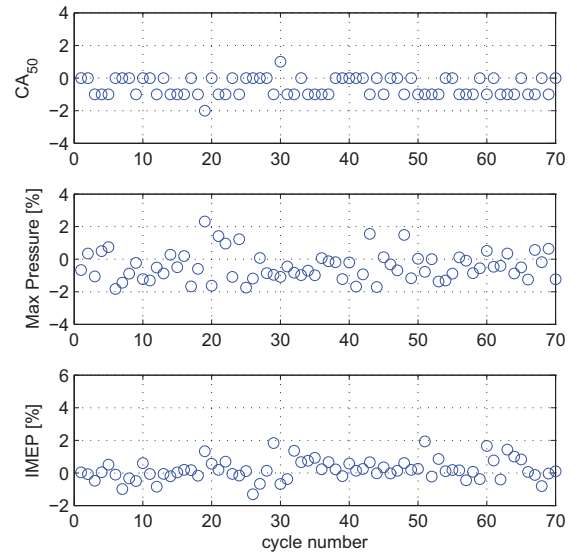

Fig. 7. Cycle by cycle error on the combustion metrics calculated from the cylinder 1 output of the augmented pressure estimator (Engine condition $N = 2000r/min, T = 40Nm$).

in-cylinder pressure traces of a multi-cylinder engine, relying on the engine crankshaft speed sensor measurement. The objective is to characterize the cylinder to cylinder pressure imbalances that result from the distribution of air and EGR to the engine cylinders, with applications to cylinder-by-cylinder closed-loop combustion control.

A sliding mode observer was initially designed based on a simple model characterizing the instantaneous indicated torque and crankshaft dynamics of a multi-cylinder Diesel engine during the closed-valve portion of the engine cycle. To improve the estimator accuracy when two cylinder pressure traces overlap, the sliding mode observer was augmented

with an additional state that represents the effects of the preceding cylinder. This allowed the estimator to provide the pressure traces of the engine during an entire cycle.

The estimator was validated against experimental data. The results, in terms of cylinder pressure traces reconstruction and calculated combustion metrics, show that the design is sufficiently accurate and robust to disturbances in the measured signals. In particular, the augmented estimator was able to remove the effect of the overlap to obtain an accurate pressure trace, which leads to an improved estimation of the pressure and *IMEP* during the entire engine cycle.

REFERENCES

[1] Guzzella, L., and Amstutz, A., 1998. "Control of Diesel Engine". *IEEE Control Systems Magazine,* **18**, pp. 53–71.

[2] Maringanti, R., Midlam-Mohler, S., Fang, M., Chiara, F., and Canova, M., 2009. "Set-Point Generation Using Kernel-Based Methods for Closed-Loop Combustion Control of a CIDI Engine". *Proceedings of the 2009 Dynamic System and Control Conference*.

[3] Fang, M., Midlam-Mohler, S., Maringanti, R., Chiara, F., and Canova, M., 2009. "Optimal Performance of Cylinder-by-Cylinder and Fuel Bank Controllers for a CIDI Engine". *Proceedings of Dynamic Systems and Control Conference*.

[4] Powell, J., 1993. "Engine Control Using Cylinder Pressure: Past, Present, and Future". *Journal of Dynamic Systems, Measurement, and Control,* **115**, pp. 343–350.

[5] Al-Durra, A., Canova, M., and Yurkovich, S., 2011. "A Model-Based Methodology for On-Line Estimation of Diesel Engine Cylinder Pressure". J. Dyn. Sys., Meas., Control 133, 031005.

[6] Rizzoni, G., 1989. "Estimate of Indicated Torque from Crankshaft Speed Fluctuations: A Model for the Dynamics of the IC Engine". *IEEE Transactions on Vehicular Technology,* **38**(3).

[7] Wang, Y.-Y., Krishnaswami, V., and Rizzoni, G., 1997. "Event-Based Estimation of Indicated Torque for IC Engines Using Sliding-Mode Observers". *Control Engineering Practice,* **5**(8), pp. 1123–1129.

[8] Chen, S., and Moskwa, J., 1997. "Application of Nonlinear Sliding-Mode Observers for Cylinder Pressure Reconstruction". *Control Engineering Practice,* **14**, pp. 1115–1121.

[9] Connolly, F., and Rizzoni, G., 1994. "Real Time Estimation of Engine Torque for the Detection of Engine Misfires". *Journal of Dynamic Systems and Control,* **116**.

[10] Lee, D., and Rizzoni, G., 1995. "Detection of Partial Misfire in IC Engines Using a Measurement of Crankshaft Angular Velocity". *SAE Paper*(951070).

[11] Guezennec, Y., and Gyan, P., 1999. "A Novel Approach to Real-Time Estimation of the Individual Cylinder Combustion Pressure for S.I. Engine Control". *SAE International Congress and Exposition*(1999-01-0209).

[12] Haskara, I., and Mianzo, L., 2001. "Real-Time Cylinder Pressure and Indicated Torque Estimation via Second Order Sliding Modes". *Proceedings of the American Control Conference*.

[13] Heywood, J. B., 1988. *Internal Combustion Engine Fundamentals*. McGraw-Hill.

[14] Ponti, F., Serra, G., and Siviero, C., 2004. "A Phenomenological Combustion Model for Common Rail Multijet Diesel Engines". *Proc. of ASME ICE Fall Technical Conference*.

[15] Canova, M., Guezennec, Y., and Yurkovich, S., 2009. "On the Control of Engine Start/Stop Dynamics in a Hybrid Electric Vehicle". *Journal of Dynamic Systems Measurement and Control,* **131**(061005).

[16] Hamedovic, H., Raichle, F., Breuninger, J., Fischer, W., Dieterle, W., and Klenk, M., 2005. "IMEP-Estimation and In-Cylinder Pressure Reconstruction for Multicylinder SI-Engine by Combined Precessing of Engine Speed and One Cylinder Pressure". *SAE World Congress*(2005-01-0053).

[17] Shiao, Y., and Moskwa, J., 1995. "Cylinder Pressure and Combustion Heat Release Estimation for SI Engine Diagnostics Using Nonlinear Sliding Observers". *IEEE Transactions on Control Systems Technology,* **3**, pp. 70–78.

[18] Moro, D., Cavina, N., and Ponti, F., 2002. "In-cylinder pressure reconstruction based on instantaneous engine speed signal". *Transactions of the ASME,* **123**, pp. 220–225.